Final Report – Phase IV

Date of Report:	December 31, 2011
Contract Number:	DTPH56-05-T-0001 – Modification 5
Prepared for:	United States Department of Transportation Pipeline and Hazardous Materials Safety Administration Office of Pipeline Safety
Project Title:	"Modeling of Magnetic Flux Leakage Sensor Dynamics on In Line Inspection Tools"

Prepared by:

Dr. Lynann Clapham
Principal Investigator
Applied Magnetics Group
Queen's University
Kingston, Ontario, Canada K7L 3N6
lynann@physics.queensu.ca

Dr. Vijay Babbar
Project Manager,
Applied Magnetics Group
Queen's University
Kingston, Ontario, Canada K7L 3N6
babbar@physics.queensu.ca

Mr. Ian Wood
Director of Programs
Electricore, Inc.
27943 Smyth Drive, Suite 105
Valencia, CA 91355
ian@electricore.org

Mr. Mark Piazza
Team Technical Coordinator
Pipeline Research Council International, Inc. (PRCI)
3141 Fairview Park Drive, Suite 525
Falls Church, VA 22042
mpiazza@prci.org

Table of Contents

1. Introduction 3
   - 1.1 Project Objectives 4

2. Finite Element Modeling, MATLAB Code and Experimental Work 6
   - 2.1 Finite Element Modeling of Defects 6
   - 2.2 MATLAB Code 11
   - 2.3 Experimental Work 15

3. Effect of Sensor Liftoff 17
   - 3.1 Modeled MFL Signals from Defects 21
   - 3.2 Experimental Sensor Liftoff Signals 26

4. Effect of Magnet Liftoff

MODELING OF MAGNETIC FLUX LEAKAGE SENSOR DYNAMICS ON IN LINE INSPECTION TOOLS

1. Introduction

The current phase (Phase IV) is an extension to the main project entitled, "Understanding Magnetic Flux Leakage (MFL) Signals from Mechanical Damage in Pipelines" co-funded by DOT PHMSA/PRCI (DTPH56-05-T-0001), and the present report is an addendum to the main project report submitted in December 2010 [1]. The main project work was aimed at development of magnetic finite element analysis (FEA) models that accurately predict the MFL signals produced by mechanical damage in pipelines. The MFL signals were obtained from defects such as gouges of various sizes and shapes and dent+gouge type of composite defects. These signals were produced at a constant liftoff of the sensor from the sample surface and contained information about the defect geometry as well as residual strains present around the defect. In practical scenario, however, the fast moving detector assembly, also known as pig, may undergo variable liftoff while traversing the defect geometry, which may introduce significant liftoff of the sensor as well as the magnet pole pieces from the sample surface, particularly near the trailing end of the defect geometry. The liftoff may cause signal loss in the liftoff region and may generate signal that is difficult to identify.

An example of a potential detector liftoff effect is illustrated below in Figures 1 and 2. At the left (Figure 1) is shown is a typical MFL (radial component) contour plot for a circular plain dent with the peaks associated with dent strain and dent geometry identified. At the right (Figure 2) is a schematic of the cross section of a dent, with the detector trajectory shown as a dotted line in red. If tool movement is from right to left as indicated, then the MFL signals from the back half of the dent will diminish or disappear as the detector loses contact with the pipe surface. Problems such as that illustrated in Figure 2 could lead to missing or misleading MFL signals which reduces the accuracy of the ILI tool result and may confuse the interpretation. In particular, signals associated with strain (which tend to be of lower magnitude than geometry-induced signals) are likely to be obscured and features such as metal loss may be misinterpreted.

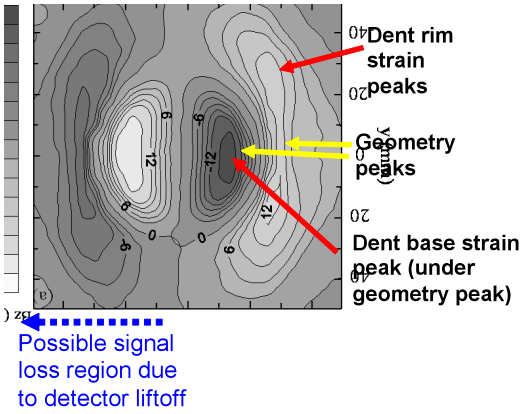

Figure 1. Typical MFL signal produced under laboratory conditions without detector liftoff

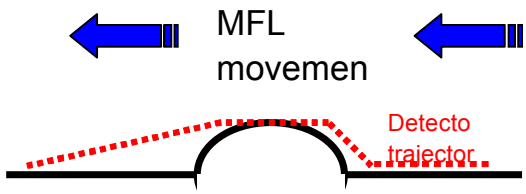

Figure 2. Schematic cross section of the MFL tool trajectory over a dent resulting in

detector liftoff

Some research groups have undertaken studies on effects of detector liftoff on MFL signal in the past. However, there has been no focused research by the pipeline industry to conduct detailed analysis of this dynamic aspect of pipeline inspection or its impact on detection, sizing, and characterization of mechanical damage features. Work by Battelle in 1999 [2] showed that detector liftoff can have significant effects on the MFL signal, however to date there have been no detector/pole piece liftoff studies for MFL signals from mechanical damage. A subsequent study by Blade Energy Partners [3] as part of a PRCI-PHMSA sponsored research project (DTPH56-06-T-000016, Project B) reported that most ILI technology vendors indicated that their technologies incorporate proprietary mechanical designs that minimize sensor liftoff when traversing plain dents less than 6% OD in depth. Their research demonstrated the capabilities of current ILI technologies to effectively detect and identify dents, but no evaluation was made with regard to sensor contact with the interior pipe wall in dents/dented regions and its effect on the corresponding signals. Also, like the Battelle study, the project did not include analysis of the impact of sensor liftoff on assessing the performance capabilities of current ILI technologies for mechanical damage detection and discrimination. Metal loss sizing and characterization of other secondary features within dents and dented regions is generally offered on a best endeavor basis.

1.1 Project Objectives

The current project builds on the magnetic finite element modeling work that has been developed for dents and gouges through the prior PHMSA-PRCI sponsored research program. The primary objective of the project is to model the effect of detector trajectory and MFL magnet liftoff for dents of varying severity. It involves modeling of realistically formed dents to provide data to fill the following existing knowledge gaps:

- The effects on the MFL signal of varying degrees of detector liftoff for a variety of plain dent shapes, sizes, and orientations (for example, circular and elongated defects in axial and circumferential orientations).
- The effects on the MFL signal of varying degrees of detector liftoff for a variety of dent+gouge shapes, sizes and orientations.
- The effects of magnet's pole piece liftoff on MFL signals for plain dents and dents+gouges.

The study will be confined to modeling effects only. Model verification will take place using MFL measurements (undertaken by the Applied Magnetics Group) on selected plain dent and dent+gouge samples obtained from other DOT-funded mechanical damage studies currently ongoing with Electricore and PRCI.

The complete work is covered in the following chapters:

- Chapter 2: Finite Element Modeling, MATLAB Code and Experimental Work: This chapter introduces the type of defects used for finite element modeling and experimental MFL measurements. It gives detailed description of the finite element modeling used to model MFL signals from various defects, and includes the procedure followed to select data points from various sets of parallel planes to simulate the detector and magnet liftoff.

- Chapter 3: Effect of Sensor Liftoff – Modeling versus Experiment: It includes modeled MFL signals for different magnitudes of sensor liftoff. The modeled signals are compared with the experimental signals from similar defects.

- Chapter 4: Effect of Magnet Liftoff – Modeling versus Experiment: This chapter shows the effect of magnet liftoff (in the absence of sensor liftoff) on MFL signal from various types of defects. The signals obtained from FEM are compared with experimental signals from defects of corresponding geometry.

- Chapter 5: Effect of Sensor+Magnet Liftoff – This chapter presents the cumulative effect of sensor liftoff and magnet liftoff on MFL signal from different defects. It also includes the corresponding experimental signals for comparison.

- Chapter 6: Conclusion: This chapter summarizes the main features of the work and highlights the conclusion drawn from the current study. It also includes recommendations for the future work.

2. Finite Element Modeling, MATLAB Code and Experimental Work

This chapter introduces the following four types of defects used in the present work:

- Plain circular dent
- Axially-oriented elongated dent
- Circumferentially-oriented elongated dent
- Axially-oriented dent+gouge

A number of defects of each type are used for this work, but only a few representative ones are included in this report. The defect samples for experimental MFL measurements are taken from the previous and concurrent projects. The defects of the similar geometry are modeled using FEM and MATLAB and the results are compared with experiment.

2.1 Finite Element Modeling of Defects

Infolytica's MagNet6 commercial software package is used for three-dimensional magnetic finite element modeling. Most of the defects exhibit two-fold symmetry, so half models were used wherever possible. A half model of a circular dent is shown in Fig. 3 along with an experimental dent of similar geometry. It consists of a 4 mm thick steel plate having a circular dent in the middle. The dent has a depth of 8 mm and its sloping wall extends from an inner radius of 12 mm to outer radius of 28 mm. Two permanent magnets of coercivity 1.6×10^{6} Am^{-1} are used to magnetize the plate in the x-direction (axial direction). This particular combination of the plate dimensions, magnet dimensions and coercivity produces a flux density of about 1.8 T in the plate, which corresponds to a high magnetization level during an actual MFL inspection.

A typical FE mesh of the plain dent model is shown in Figure 4. It consists of 80,255 tetrahedral elements with a mesh tolerance of 1.008×10^{-7}. Normal flux boundary conditions are used on the outer left and right faces of the magnets. The presence of mechanical stresses is ignored in the current work. The 'no lift' MFL signal is measured at a distance of 1 mm from the inside convex geometry of the defect where the sensor is supposed to lie during an actual MFL inspection. The signal from the convex surface is obtained by considering MFL data from a set of parallel planes underneath the plate and then selecting the points adjacent to the defect geometry. A MATLAB code is used to pick the required data points and sort them out to obtain a useful signal, as described in the next Section.

The elongated dent used in the present work is shown in Figures 5 and 6 along with its FE model. It has a length of 64 mm, width of 32 mm and a depth of 8 mm. This defect is studied in two different orientations – axial orientation and circumferential or hoop orientation. Figure 5 shows the FE model in the axial orientation, where the magnetic field is applied along the length of the defect. In the circumferential orientation (Figure 6), the defect is rotated by 90°, so the direction of magnetic field is perpendicular to the length of the defect.

The MFL signal from defects of the type dent+gouge will be affected by sensor liftoff only if the dent is severe enough to modify the inner wall geometry. We used an X70 pipeline sample coupon having a backhoe created dent+gouge from an industry. The defect has significant inner wall dent geometry to make it suitable for the current study. This 6.5 mm thick sample (Figure 7) has an elongated dent of length 145 mm, average width 24 mm, and a

maximum depth of 13 mm. This defect is named as ‘Gouge 1’. A detailed physical examination of the dent helped us determine the following dimensional constraints for the modeling work:

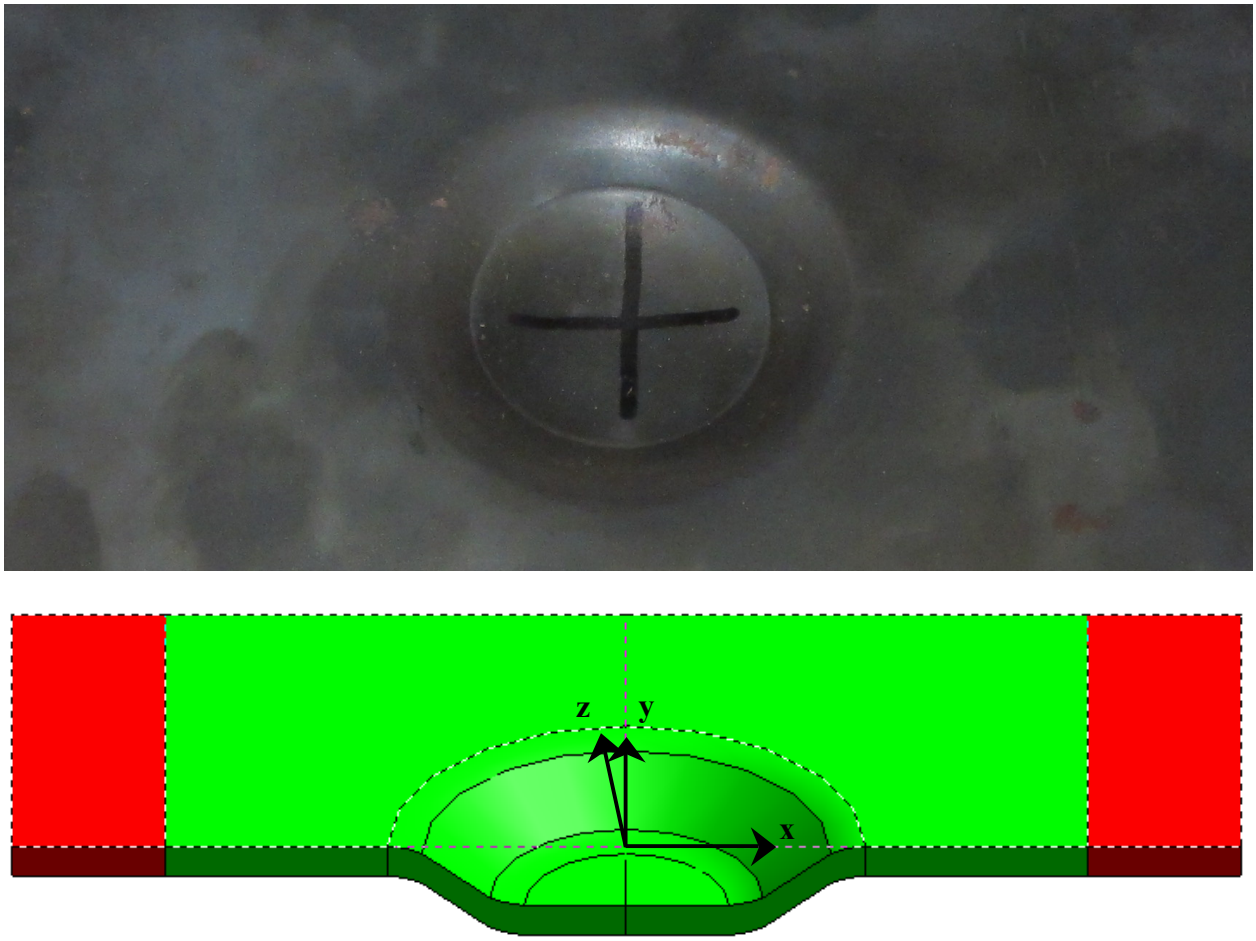

Figure 3. Experimental circular dent (top); Finite element model of the circular dent (bottom). Magnet pole pieces (red blocks) produce magnetic flux in the x-direction (axial direction).

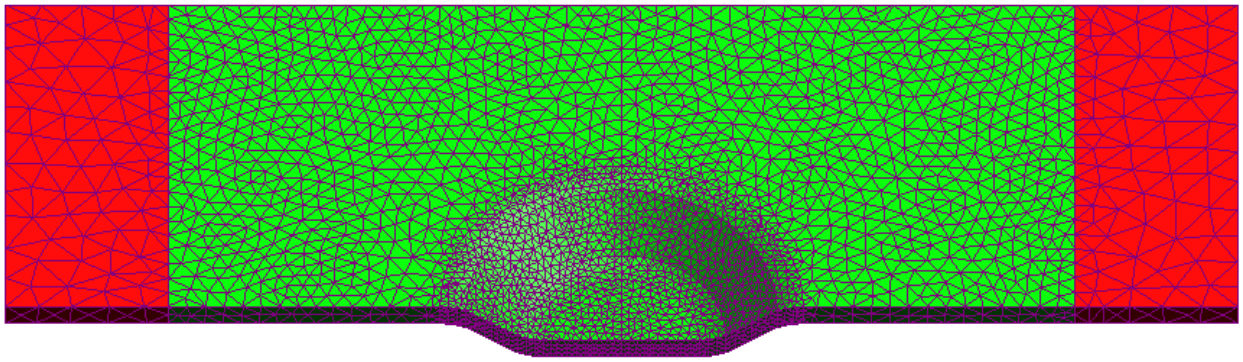

Figure 4. Finite element mesh of the circular dent model shown in Figure 3.

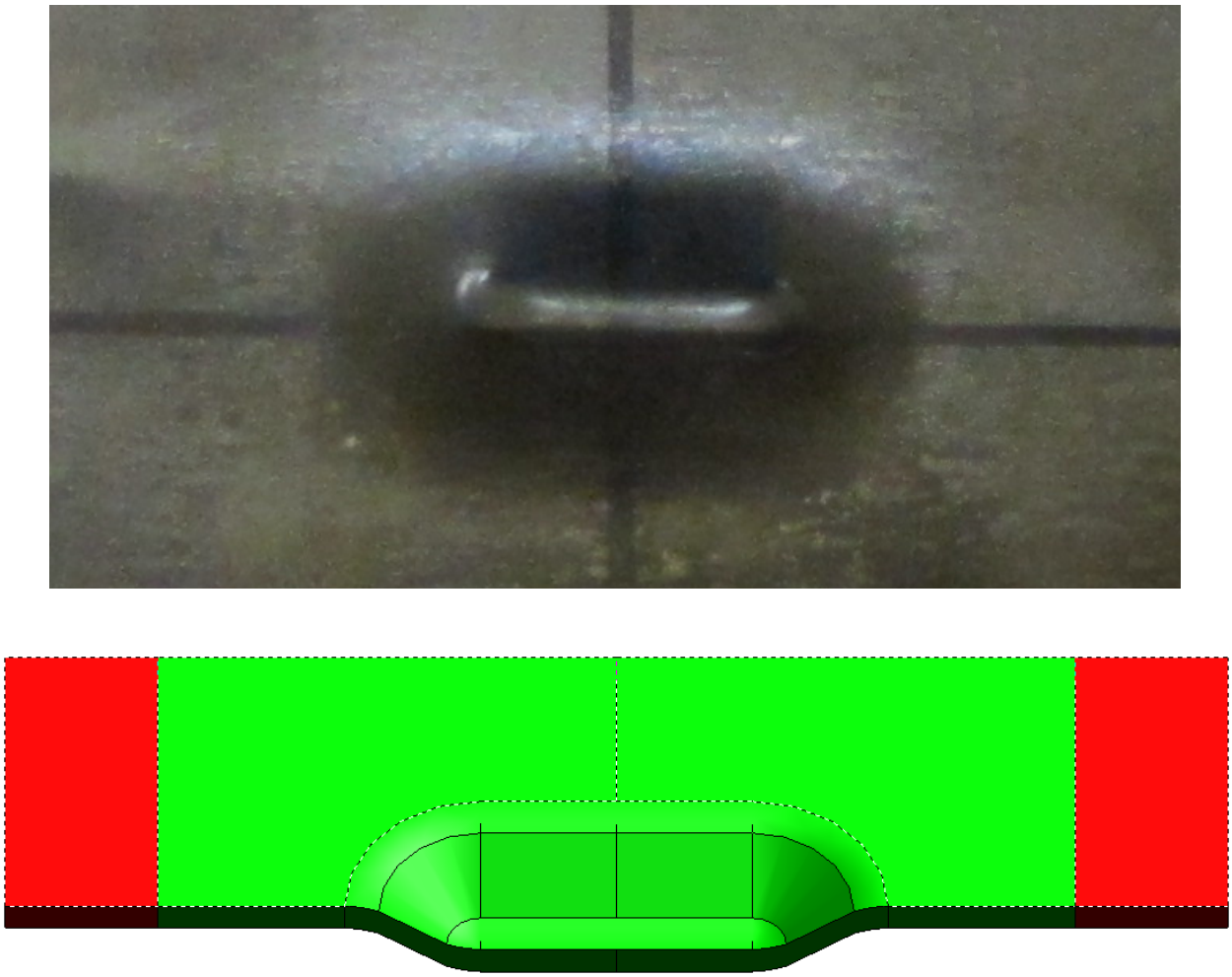

Figure 5. Experimental axially-oriented elongated dent (top); Half FE model of the above dent (bottom). Magnet pole pieces (red blocks) produce magnetic flux in the axial direction.

1. The topside (outer pipe wall) cross-section of the dent is essentially rectangular except for a variation in the width. The topside edges are blunt and the inside corners are round along the length of the dent. The underside (inner pipe wall) of the dent has an elongated round shape, which is quite similar to that of our earlier elongated laboratory dents of comparable size.

2. The plate thickness is non-uniform in the dented region; the variation in thickness is estimated to be ±1-2 mm.

3. The dent is broadly symmetrical across an axial plane normal to the pipe wall and dividing the width in two halves, thus making it possible to work with a half model with two-fold symmetry.

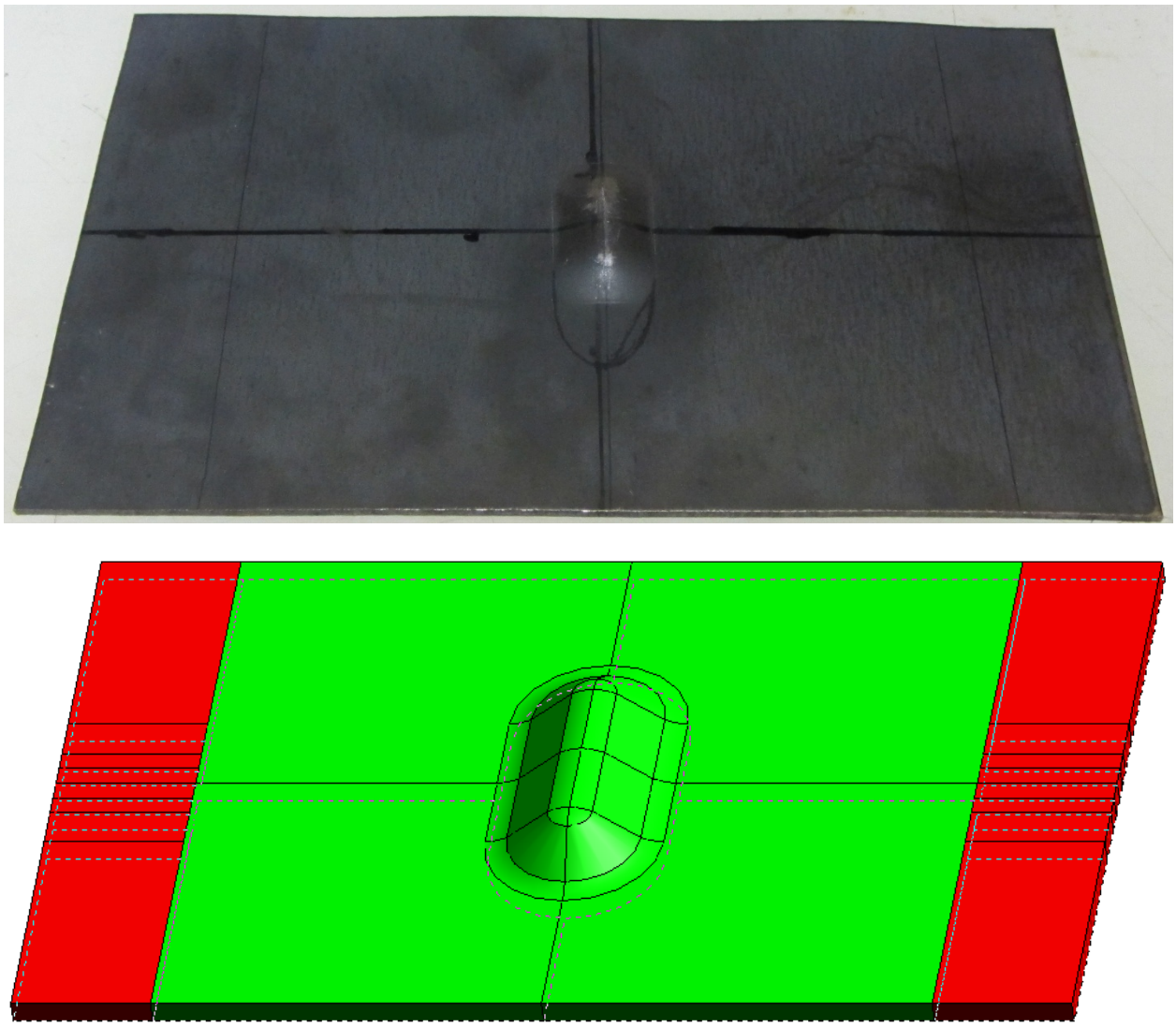

Figure 6. Underside of an experimental circumferentially-oriented elongated dent (top), and full FE model of the above dent (bottom). Magnet pole pieces (red blocks) produce magnetic flux in the axial direction.

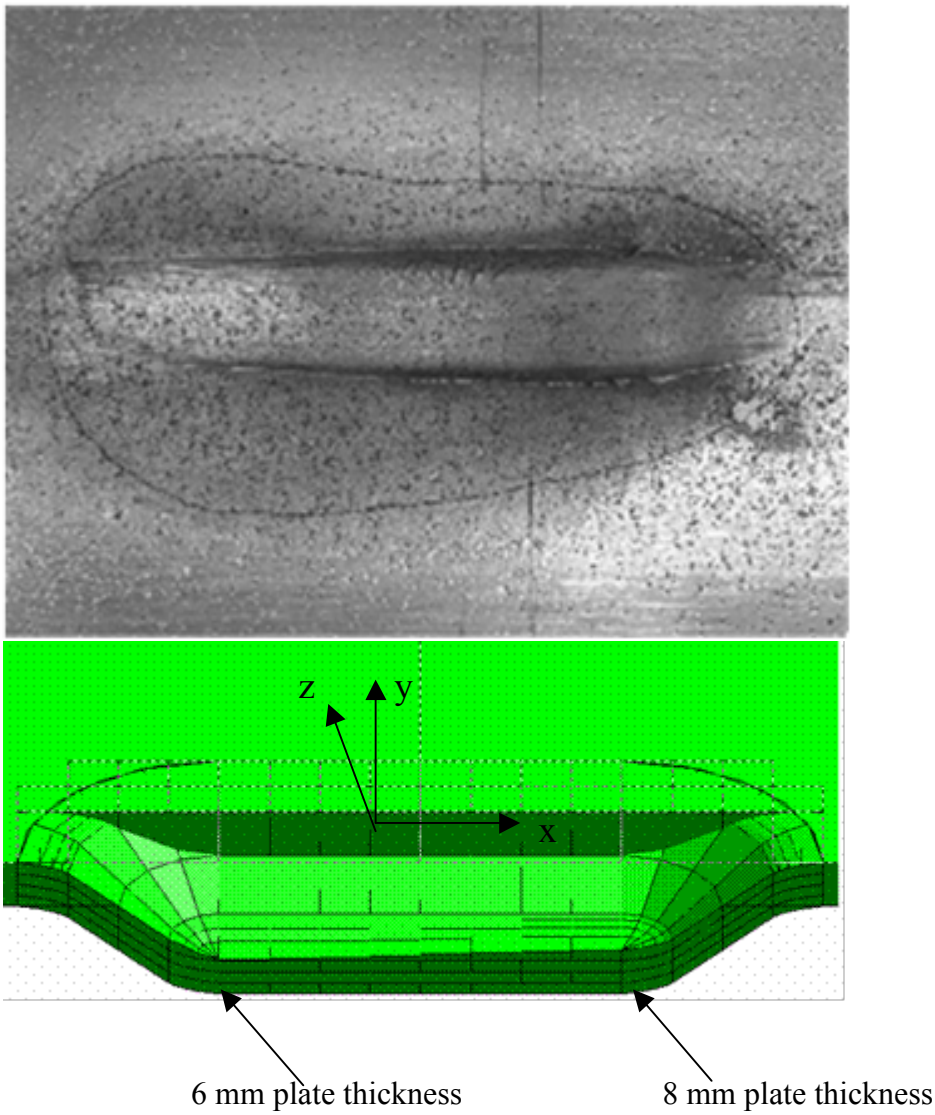

Figure 7. A pipeline backhoe dent+gouge coupon, called 'Gouge 1' in this work (top); Half-section of the FE model of the above defect with gradually changing base thickness as well as depth and having different sidewall slopes near the depressions on the two sides (bottom).

Since a dent+gouge defect, in general, has an asymmetric geometry, it is very difficult to accurately model an experimental gouge. The modeling of the experimental dent+gouge is, therefore, accomplished in two parts, a) modeling a symmetric defect, and b) adding asymmetry to depth and sidewall slope. Figure 6 shows the model of dent+gouge defect. It consists of a plate of dimensions 176 mm × 108 mm × 8 mm having a rectangular defect cross-section of 128 mm × 16 mm with a maximum depth of 16 mm. To introduce asymmetry into the defect depth and steepness of the side walls, the sections of the top layer were resized to make a stepladder with a step size of 0.25 mm, thus producing a model of variable base thickness and pit depth. The thickness of the base plate near the left side of the dent is 6mm, which is 2mm less than the thickness near the right side. The presence of mechanical stresses is ignored in this model.

Although the left half of this dent+gouge model is not a mirror image of the right half, the model still has a uniform width throughout, which allows the use of two-fold symmetry instead of four-fold. The xz plane is the plane of symmetry in this model. The patterns obtained from this half model can be mirrored in the xz plane to simulate the full MFL pattern. The minimum mesh size used in the dented region is 2 mm. The H_x field inside the plate is about 30,000 A/m just outside the dented region and about 22,000 A/m in the base region underneath the dent.

Finally, the model of another dent+gouge defect, named as 'Gouge 2', used in the present study is shown in Figure 8. This model represents severe gouging with high degree of asymmetry and simulates the cumulative effect of dent geometry, wall thinning and metal loss. The gouge has a length of 130 mm, a variable width of 0-10 mm, and a variable depth of 0-8 mm. This defect is studied only by finite element modeling.

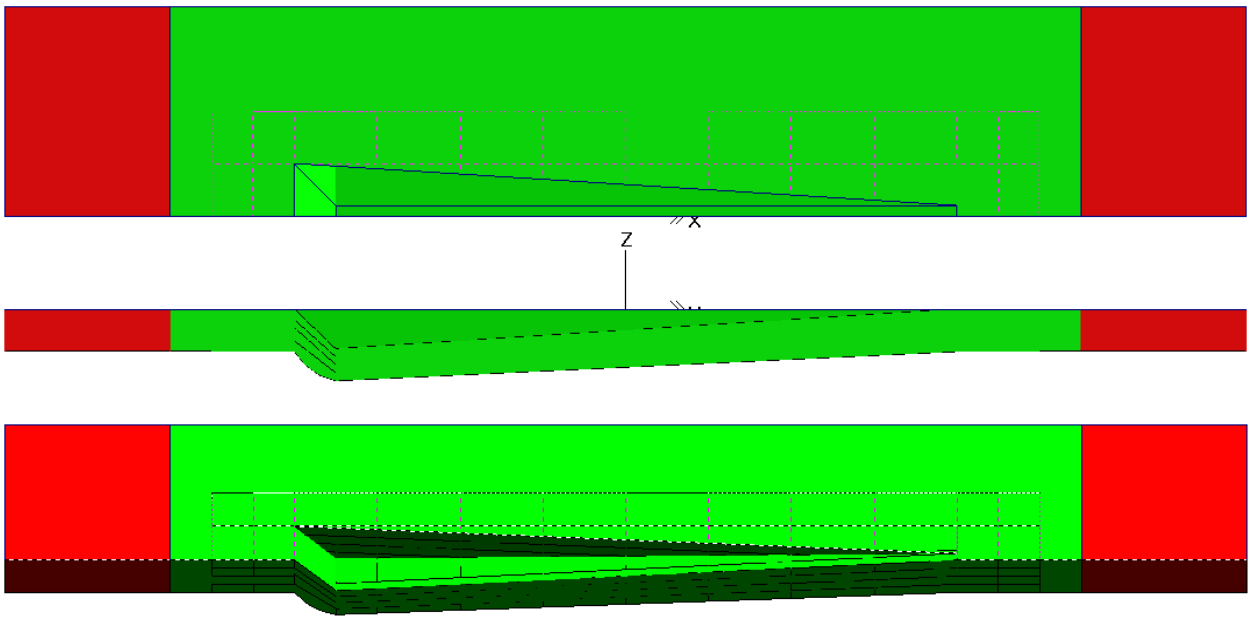

Figure 8. Topview, sideview and 3D-view of half-model of a severely deformed dent+gouge, called 'Gouge 2'in the present work.

2.2 MATLAB Code

Infolytica's MagNet software can generate values of magnetic flux at any particular point, line, or plane in Cartesian coordinates within the boundaries of the solved model. One can also use an in-built MagNet script to obtain three flux components (axial, radial, and circumferential) on a number of parallel planes along x, y or z direction. However, it is not straightforward to pick these flux component values along a curved surface, such as the inner wall curvature of a dent or a gouge, especially for complex defect geometries. We accomplished this in two steps: a) determining the coordinates of the points using defect geometry, and b)

using a MATLAB script to pick the corresponding magnetic flux component values from a set of parallel planes obtained from a solved model.

A typical MATLAB code, called PICKOUT, used to pick relevant flux component values from a set of any number of parallel planes is given below. The data points from each plane are stored in separate files and all the file names are stored in another file, called file_table, which is accessed by the PICKOUT code. Separate MATLAB codes were written for picking flux values from circular dent, elongated dent, and dent+gouge defects.

Sample MATLAB Script:

```
% 'PICKOUT' is a matlab script file.
%
% This script copies datasets from various data file in to a master file.
% All the data contained in the data and master files are x/y/z/value sets
% and all the files have the same amount of values.
%
% The function needs a file_table file, which contains the complete
% filename of the master file in the first row, followed by all the data
% files. Every data file needs also a data point file with the suffix '_dp'.
% Every row of the data point file contains x/y/z numbers of the wanted data.
% This datasets will be copied to the master file.
%
% The changed master file will be stored in a file with the same name as the
% master file but with the suffix '_res'.
%
% All files used with this script are ASCII text files. No headers or
% '.' within the filenames are allowed. Each column shall be separated
% with a 'tab'.
%
% Author: Vijay Babbar
% Date: August 2011
% Contact: babbar@queensu.ca


% Example of file names:
%   - file_table.txt
%       Rows with the master filename in the 1st and the data filenames in
%       following.

%   - Master_dat.txt
%       Contains rows of x/y/z/value sets, which shall be partly changed with rows
%       from data files.
```

```
%
%   - data_1.txt
%       Contains rows of x/y/z/value sets, which shall be partly copied to the
%       master file.
%   - data_1_dp.txt
%       Contains rows of x/y/z data points which shall be copied from the data
%       file to the master file.
%
%   - Master_dat_res.txt
%       Contains rows x/y/z/value sets of the changed master file.

clear all
close all

%#Loading the file_table which contains all the file names wich shall be
%combined
file_table = input('Input data file name (default file_table.txt): ','s');
if isempty(file_table)
    file_table = 'file_table.txt';
end
disp(['File table ',file_table,' contains the following files:'])
% Reading the file names out of the file
files = textread (file_table,'%s','delimiter','\n')

%#Loading the data (each row contains x/z/z/data)
maindata = load (files{1});
disp(['Main data file is loaded: ',files{1}])
FileSize = size(maindata)

for n=2:length(files)

    actualfile = files{n};

    %#Loading the data (each row contains x/z/z/data)
    data = load (actualfile);
    disp(['Data file is loaded: ',actualfile])
    FileSize = size(data)

    %#Loading the pickout table for the wanted data (each row contains x/z/z)
    %combining the file name for the pickout file
```

```
   pick_file = [actualfile(1:(findstr (actualfile,'.')-1)),'_dp.txt'];
   xyzpoint = load (pick_file);
   disp(['Pickout file is loaded: ',pick_file])
   FileSize = size(xyzpoint)

   %creating a locator vector
   location = zeros (length (data),1);

   %#searching for x/y/z coordinates
   for i=1:length(xyzpoint)
      %find corresponding row in the data
      xcoord = data(:,1) == xyzpoint(i,1);
      ycoord = data(:,2) == xyzpoint(i,2);
      zcoord = data(:,3) == xyzpoint(i,3);

      %add the location to the locator vector
      location = or(location, (xcoord.*ycoord.*zcoord));
   end
   %#Gather the data
   locator = find (location);
   disp('The following data was picked out of the data file:')
   data (locator,:)
   maindata(locator,:)  = data (locator,:);

end


%#Store data in file
% Generate filename for saving
actualfile = files{1};
savefile = [actualfile(1:(findstr (actualfile,'.')-1)),'_res.txt']
fid = fopen(savefile,'wt');
% Write the data into the file
fprintf(fid,'%6.2f; %6.2f; %6.2f; %12.8f\n',maindata');
fclose(fid);
disp (['Data stored in: ', savefile])
FileSize = size(maindata)
```

2.3 Experimental Work

Experimental MFL measurements are made on the samples shown in Section 2.1 to verify the modeling results. The experimental set-up consists of a defect sample placed between the pole pieces of a NdFeB permanent magnet circuit as shown in Figure 9. The convex surface of the dent geometry, which is equivalent to the inner wall in a real pipeline scan, is used for making MFL measurements. A Hall probe attached at the end of a detector arm scans the defect surface with a resolution of 1mm × 1mm and is operated through a LabView program. A three-dimensional plotting software (Surfer 10) from Golden Software is employed for obtaining surface and contour maps.

To simulate the detector fly-off, the sensor is assumed to be pressing against the pipe wall by means of a spring while moving with a certain speed. When the detector rides over the dent at high speed, it loses contact with the pipe wall while moving down the slope, thus causing a variable liftoff that depends on the detector speed as well as the spring constant. In the present work, the detector is assumed to be moving with a constant speed of 4 m/s, which is the typical detector speed in a real MFL inspection, and three arbitrary values of spring constant (40, 80 and 120 N/m) are used to generate three different liftoff trajectory, which will be described in Chapter 3.

Experiments to investigate the effect of magnet liftoff are set up in such as way that only the central part of the pole pieces touches the sample and the air gaps are introduced near the sides. The liftoff is introduced beneath one of the pole pieces only. The magnet liftoff is numerically estimated in terms of 'discontinuity fraction', which is defined as the fraction of the total area of the magnet pole piece that is subject to liftoff. The present work uses two values of discontinuity fraction – 0.3 (30%) and 0.5 (50%). The liftoff is produced by using steel spacers in the middle region and non-magnetic spacers on the sides.

The MFL signal recorded from various defects comprises of two components – axial component (B_x) which is in the direction of the applied magnetic flux, and radial component (B_z) which is perpendicular to the direction of the magnetic flux as well as the sample surface. The experimental results are used for comparison with the modeling results.

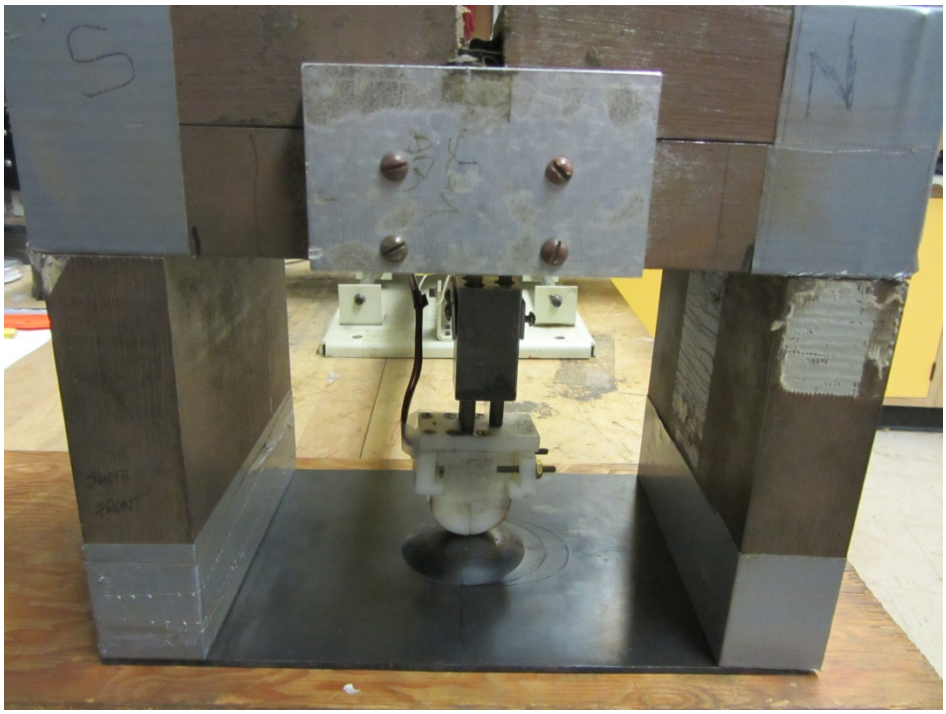

Figure 9. Experimental set up used for measuring MFL signal. The detector rides over the convex surface of the dent, which is equivalent to an inner wall scan in a real pipeline inspection.

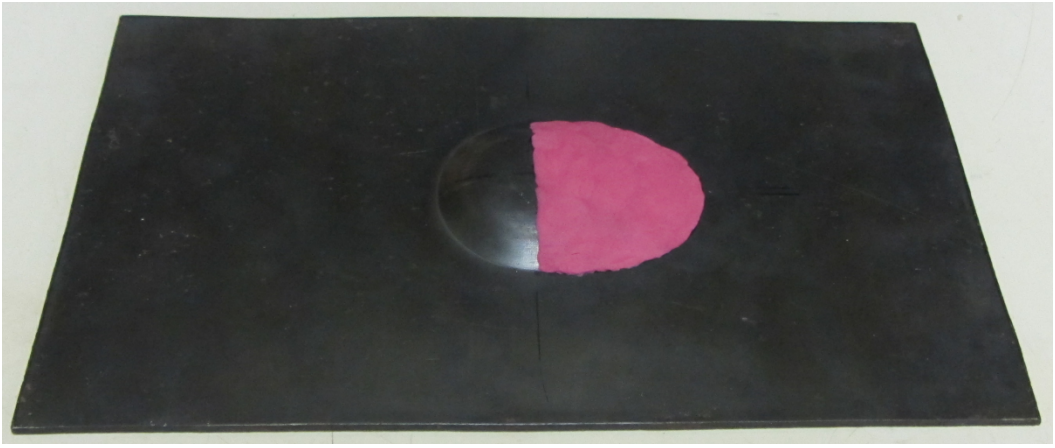

Figure 10. A dented sample used to investigate the effect of detector liftoff on MFL signal. Molding clay is used to raise the detector trajectory on half side of the dent.

3. Effect of Sensor Liftoff

In the present work, the detector is assumed to be pressing against the inner pipe wall by means of a spring while grazing the dent-free surface at a uniform constant speed of 4 m/s and a constant liftoff of 1 mm. However, it loses contact near the dent edge and may fly off over the dent slope region. The magnitude of liftoff depends on the speed of the detector, elastic constant of the spring, and the initial height (or depth) of the dent edge. Since the speed is assumed to be constant in the present work, the liftoff depends only on the initial height and the spring constant. Figure 11 shows three different central line trajectories A, B, and C produced using an initial height of 13 mm and three spring constants of 120, 80 and 40 N/m respectively. The largest liftoff occurs for the lowest value of spring constant. The liftoff is the highest for trajectory C and lowest for A. Similar trajectories were produced along off-center lines where the initial height gradually decreases from 13 mm to 6 mm, producing a range of liftoff values which are stored as an Excel file and used for picking the flux values at those locations. Since the circular dent and elongated dent have the same initial depth, the liftoff trajectories for these two cases are similar. For composite dent+gouge defect, however, the trajectory may vary due to non-uniform dent depth along the length of the defect. This chapter presents the MFL signal patterns from defects for the cases of 'No sensor liftoff' and 'Sensor liftoff' in the absence of magnet liftoff.

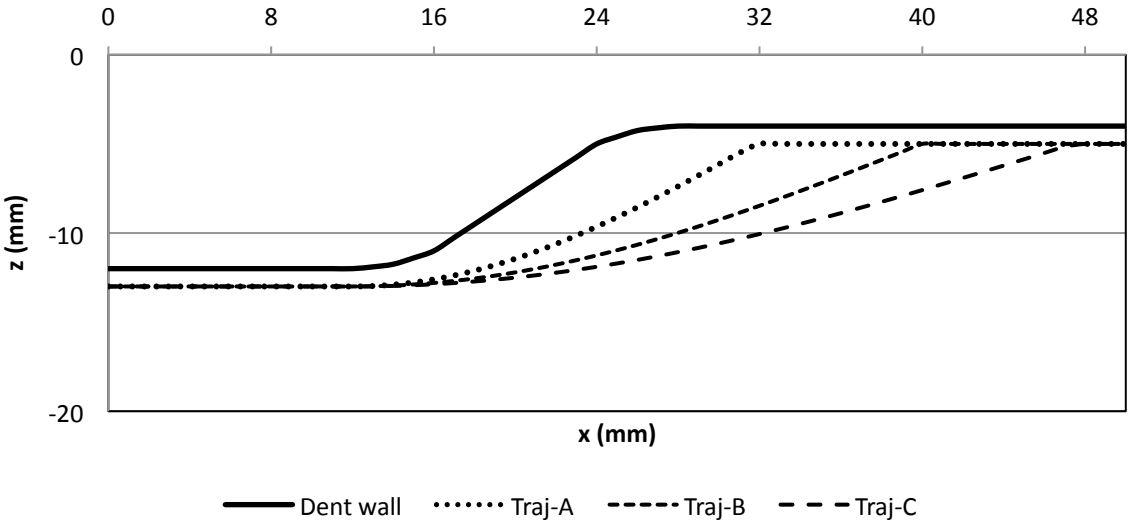

Figure 11. Cross-section of a half dent along with three different detector liftoff trajectories (A, B and C) along the center line on the convex side of the dent. The detector travels from left to right.

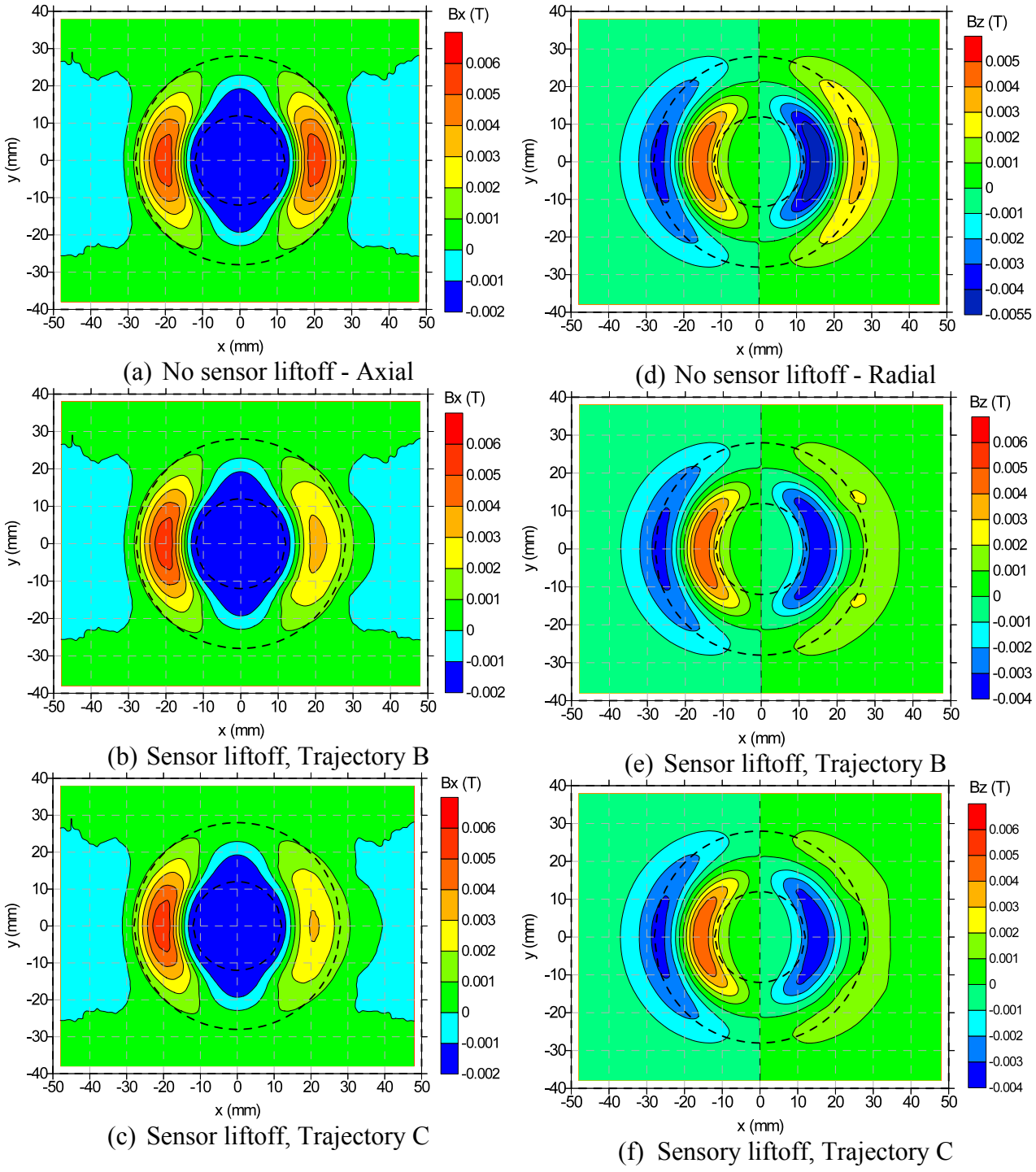

Figure 12. Inner wall MFL axial (left column) and radial (right column) contour maps of circular dent (Figures 3 and 9) produced by FEM for 'No sensor liftoff' and 'Sensor liftoff' cases. The

sensor motion is from left to right.

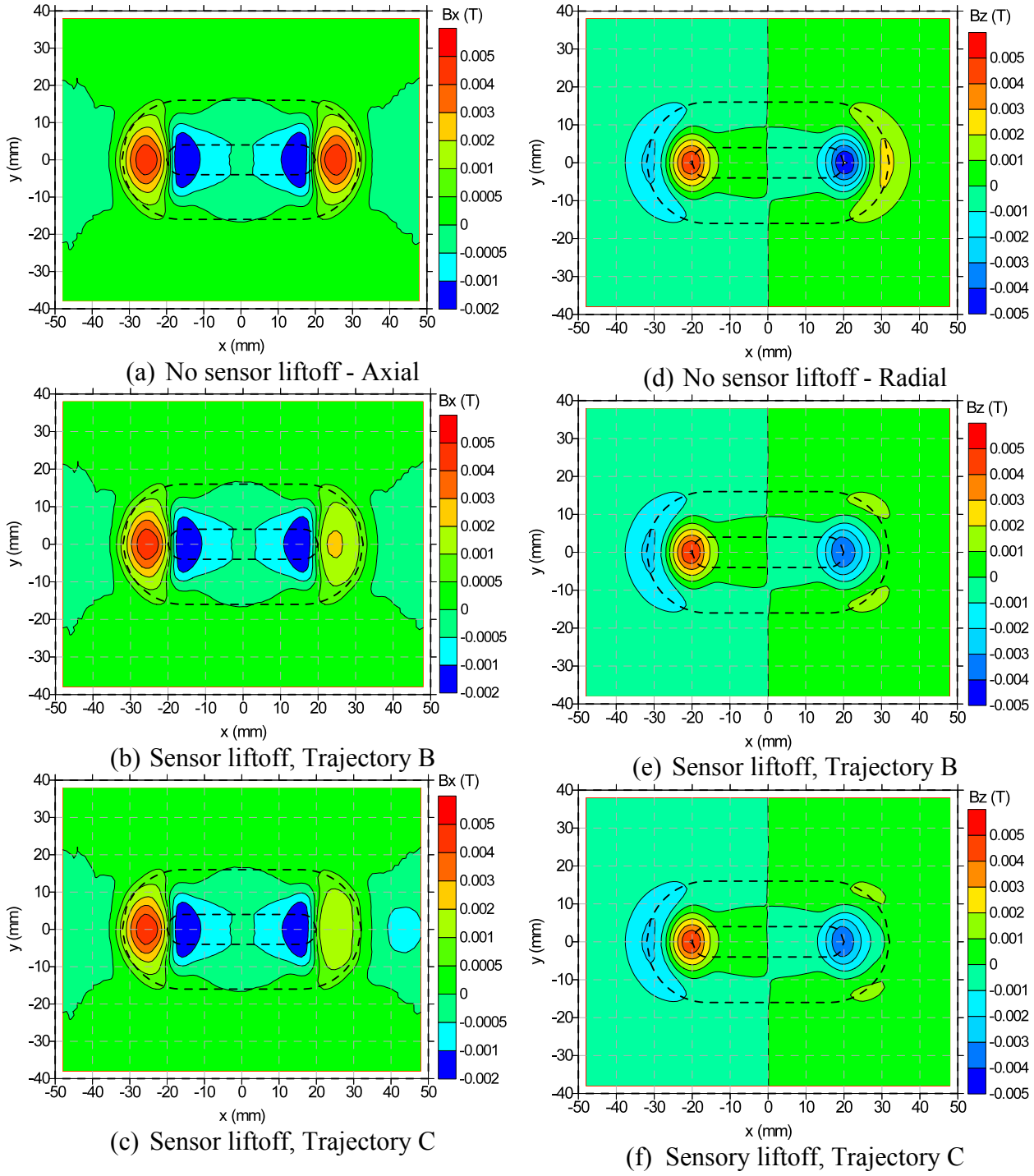

Figure 13. Inner wall MFL axial (left column) and radial (right column) contour maps of elongated dent produced by FEM for 'No sensor liftoff' and 'Sensor liftoff' cases. The sensor motion is from left to right.

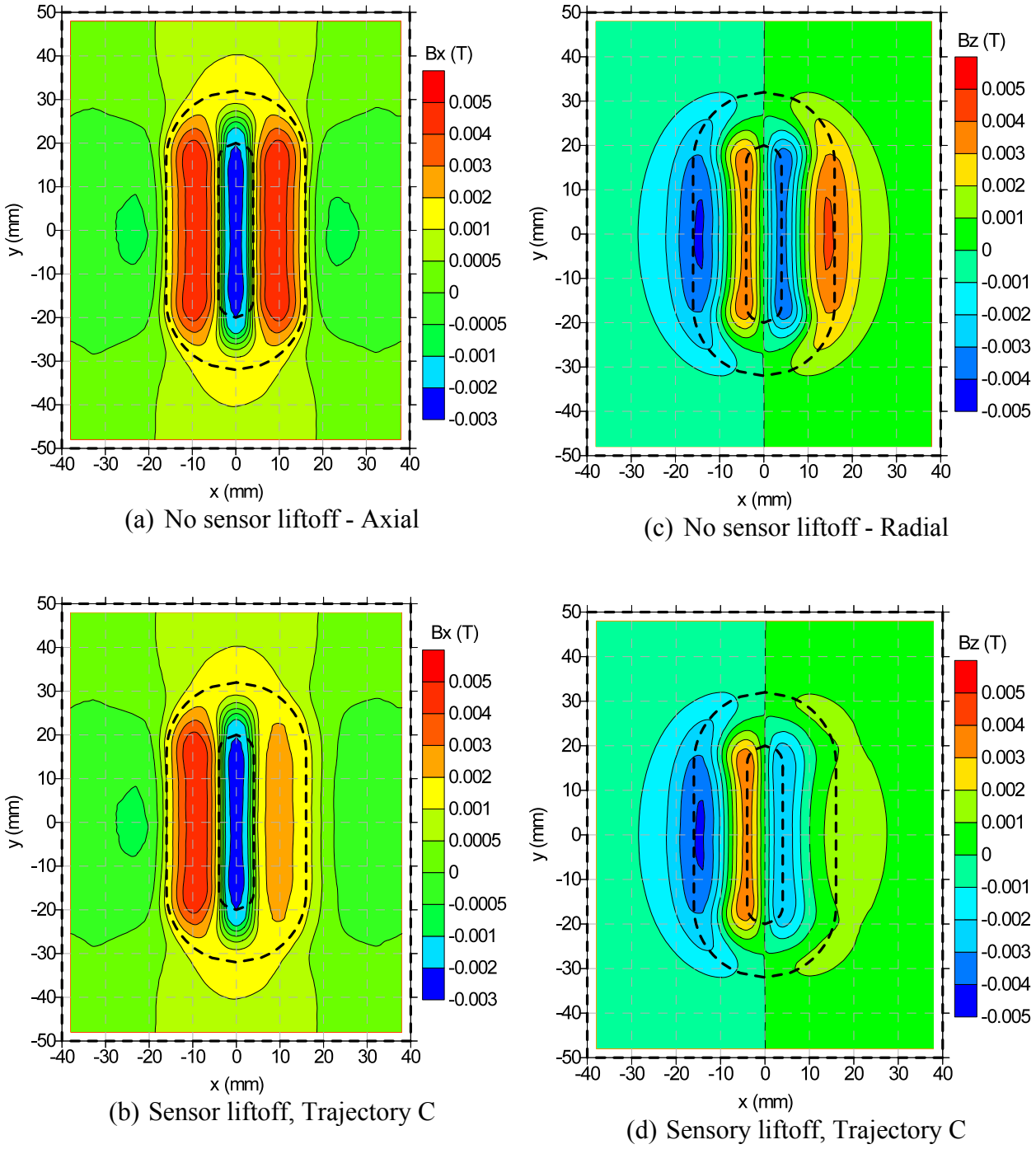

Figure 14. Inner wall MFL axial (left column) and radial (right column) contour maps of elongated dent in the circumferential (hoop) direction produced by FEM for 'No sensor liftoff' and 'Sensor liftoff' cases. The sensor motion is from left to right.

3.1 Modeled Sensor Liftoff Signals from Defects (No Magnet Liftoff)

Modeled MFL 'Sensor liftoff' signals showing the effect of detector liftoff from the defects presented in Section 2.1 are shown in Figures 12 through 16, which also include the corresponding 'No sensor liftoff' signals for comparison. Two liftoff trajectories (B and C) are used for the circular dent, while only C is used for other defects. The MFL axial signal from a circular dent has a characteristic broad central peak and two outer peaks of opposite polarity making a halo, while the radial signal is characterized by four peaks of alternate polarity, as shown in Figure 12. For axially elongated dent, however, the broad central peak in the MFL axial signal is split up into two peaks, which lie near the end regions. The nature of MFL signal for circumferentially elongated central region is almost similar to the circular dent except that the peak regions are very thin and stretch more along the circumferential direction.

In general, the sensor liftoff is found to weaken the signal for both axial and radial cases, but the radial signal appears to be affected somewhat more than the axial. In some cases the radial outer peak at the trailing end is almost wiped out due to liftoff and will be barely noticeable in real pipeline MFL scans, thus posing difficulty in defect identification. In the axial signal, the central peak is not affected by the liftoff, but the side peak near the trailing end is weakened significantly.

Finally, the MFL signal from the two dent+gouge type of defects (Gouge 1 and 2) used in the present work are shown in Figures 15 through 18. As described previously, the 'Gouge 1' (Figure 7) has significant inner wall dent geometry with variable dent depth (maximum 13 mm) and variable dent base thickness (left side is slightly thinner than the right side), as observed in a typical gouge. However, there is not much variation in the width, so a constant width is used in the model making this defect symmetrical across an axial plane normal to the pipe wall. The second dent+gouge model uses a severe gouge with high degree of asymmetry in depth and width to simulate the cumulative effect of dent geometry, wall thinning and metal loss.

The underside axial and radial MFL contour maps of 'Gouge 1' are shown in Figures 15 and 16 respectively for both 'No sensor liftoff' and 'Sensor liftoff' cases. Both the axial and radial patterns are clearly asymmetric near the two corners of the base even for the 'no lift' case, which is because of the asymmetry in depth and base thickness introduced in the model. When combined with liftoff effect on the right hand base corner, both the signals tend to become weak; the axial signal shows weakening of the outer peak and appearance of a new one of opposite polarity outward, and the radial signal losing the outer peak completely. The gouge models used in the present work do not simulate strain effects.

The MFL axial and radial patterns from 'Gouge 2' defect is shown in Figures 17 and 18.The signal is mainly observed near the left end of the gouge where the depth is maximum. The sharp little blue region on either side of the axial line appear near the corners. There are no strains in this gouge. Since dent geometry exists on the left side, the sensor motion in this case is modeled from right to left. Both the axial and radial signals diminish as a result of liftoff, as observed in other defects, and the effect is more pronounced on radial signal.

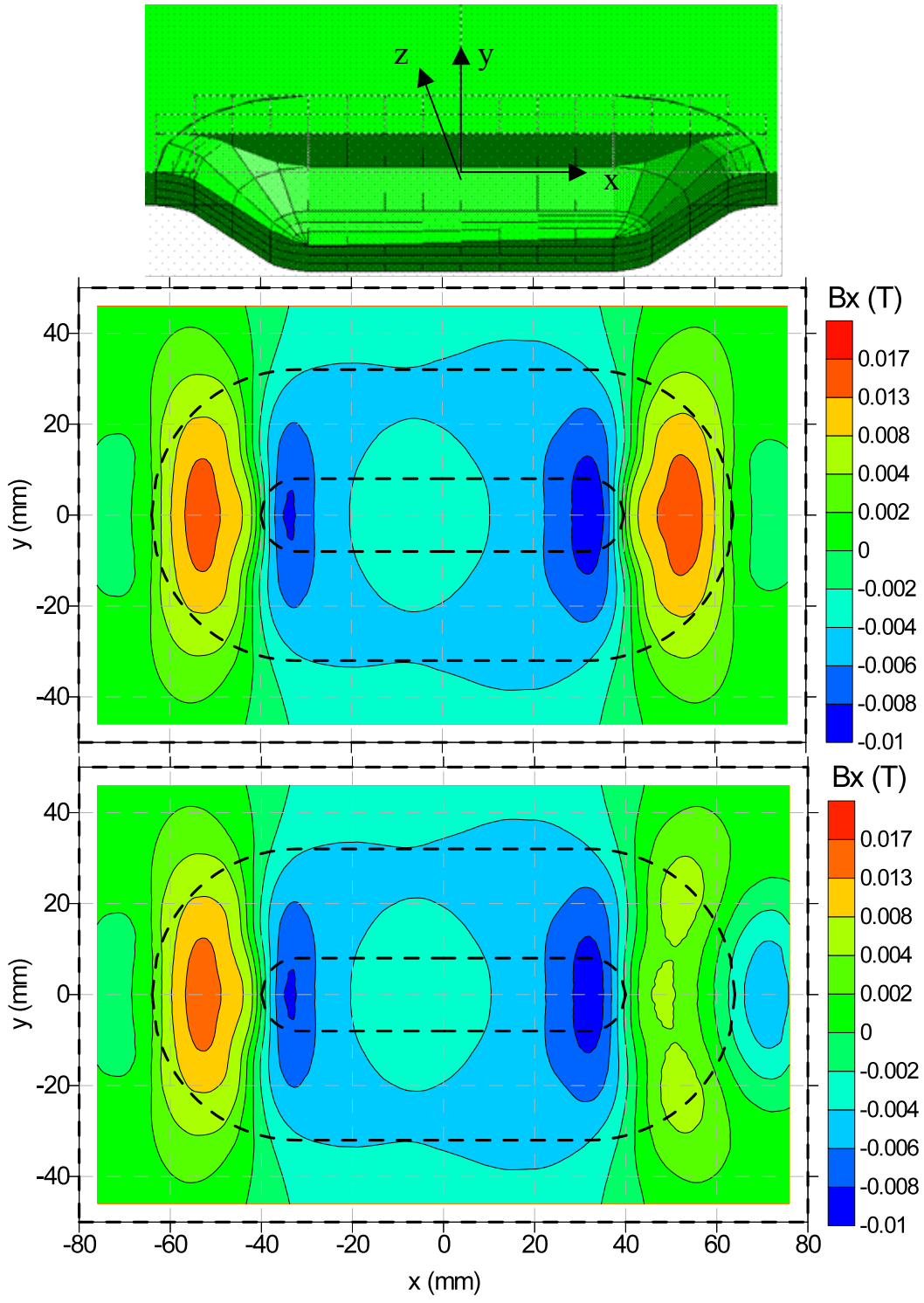
z
y
x
Bx (T)
0.017
0.013
0.008
0.004
0.002
0
-0.002
-0.004
-0.006
-0.008
-0.01
y (mm)
40
20
0
-20
-40
Bx (T)
0.017
0.013
0.008
0.004
0.002
0
-0.002
-0.004
-0.006
-0.008
-0.01
y (mm)
40
20
0
-20
-40
-80
-60
-40
-20
0
20
40
60
80
x (mm)

Figure 15. Axial gouge+dent model (top); 'No sensor liftoff' inner wall axial MFL signal (middle); 'Sensor liftoff' inner wall axial MFL signal (bottom). Sensor travels from left to right

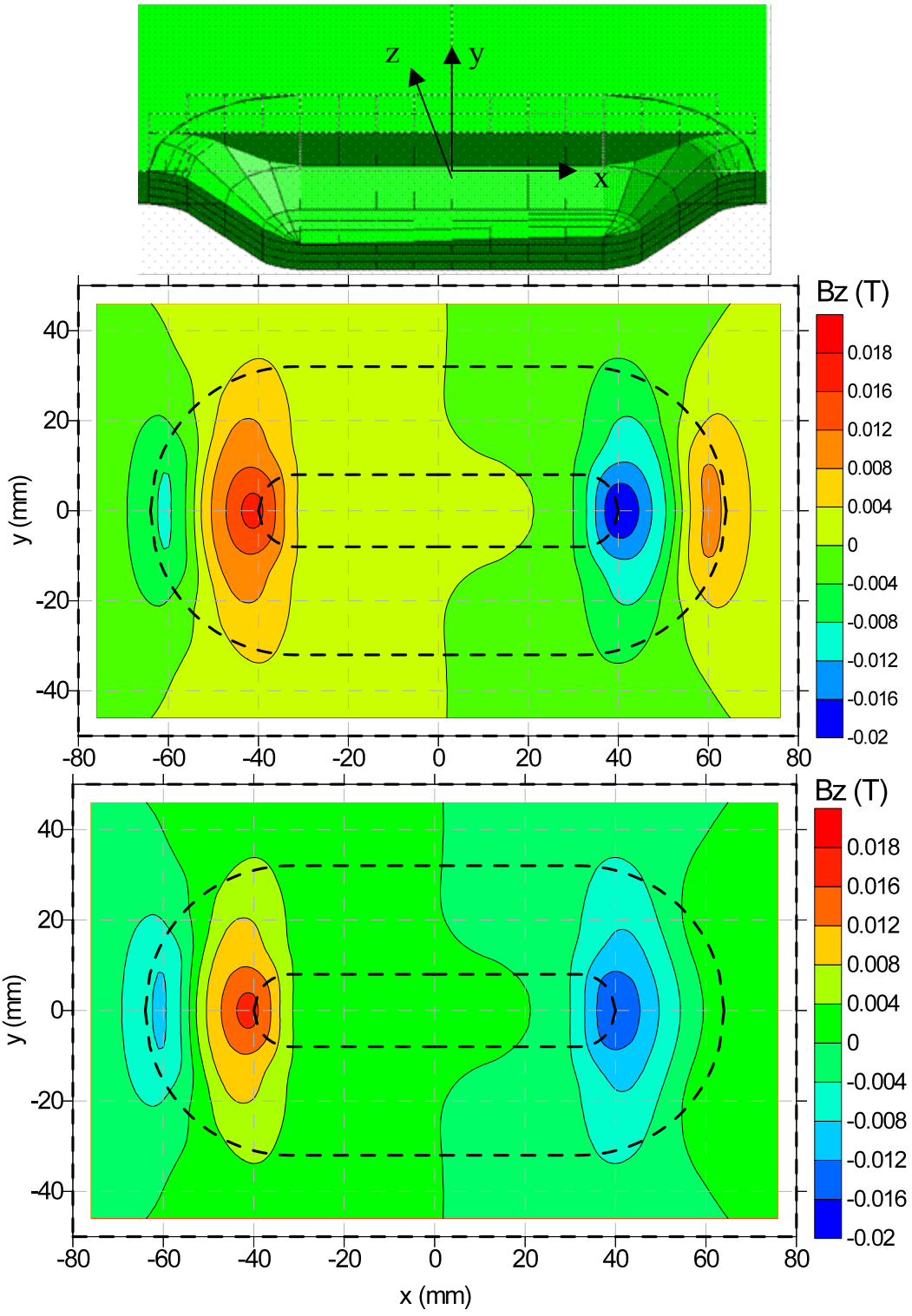

Figure 16. Radial gouge+dent model (top); 'No sensor liftoff' inner wall axial MFL signal (middle); 'Sensor liftoff' inner wall axial MFL signal (bottom). Sensor travels from left to right

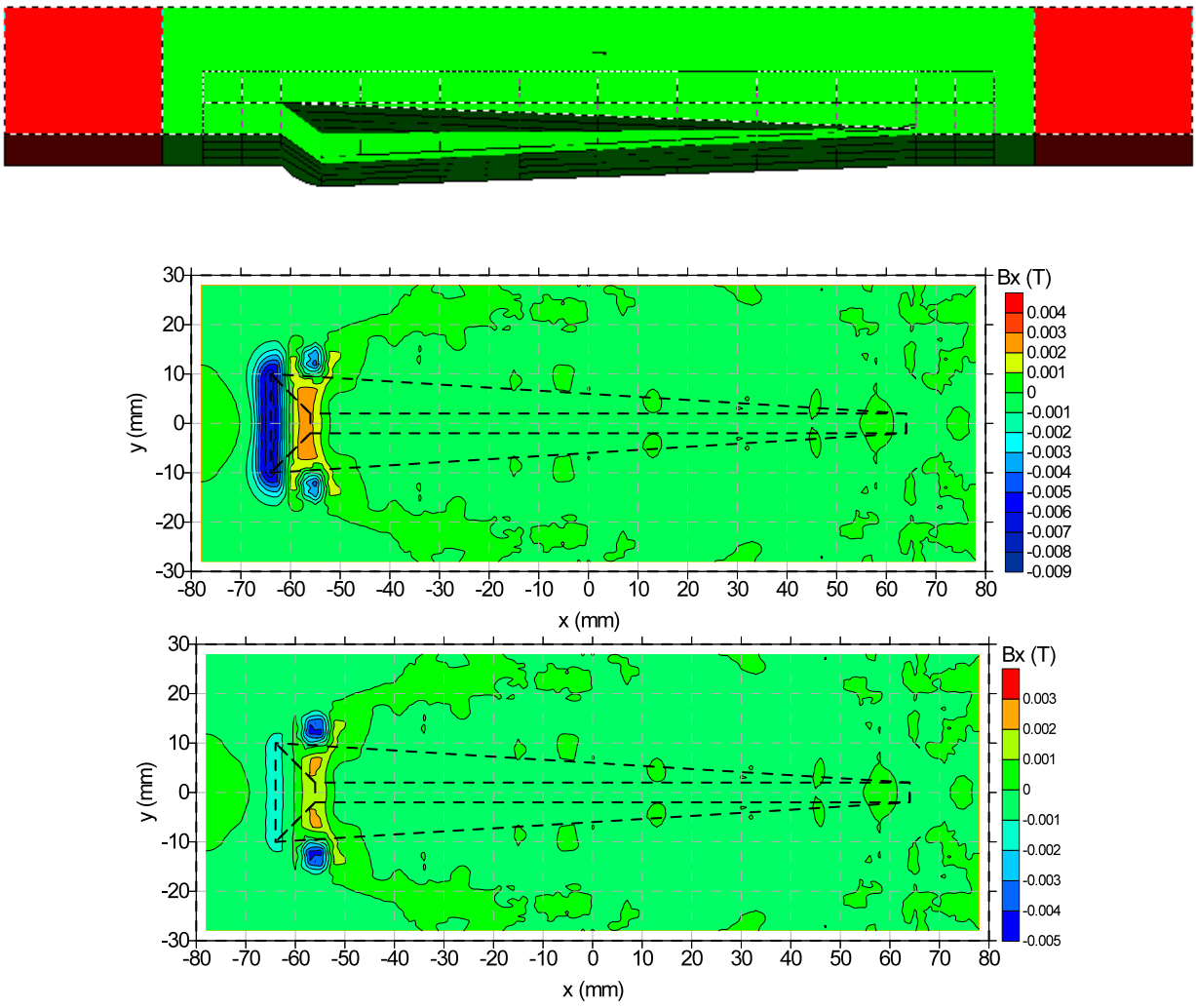

Figure 17. Half model of an axially oriented gouge+dent, called 'Gouge 2' (top); 'No sensor liftoff' inner wall axial MFL signal (middle); 'Sensor liftoff' inner wall axial MFL signal (bottom). Sensor travels from right to left.

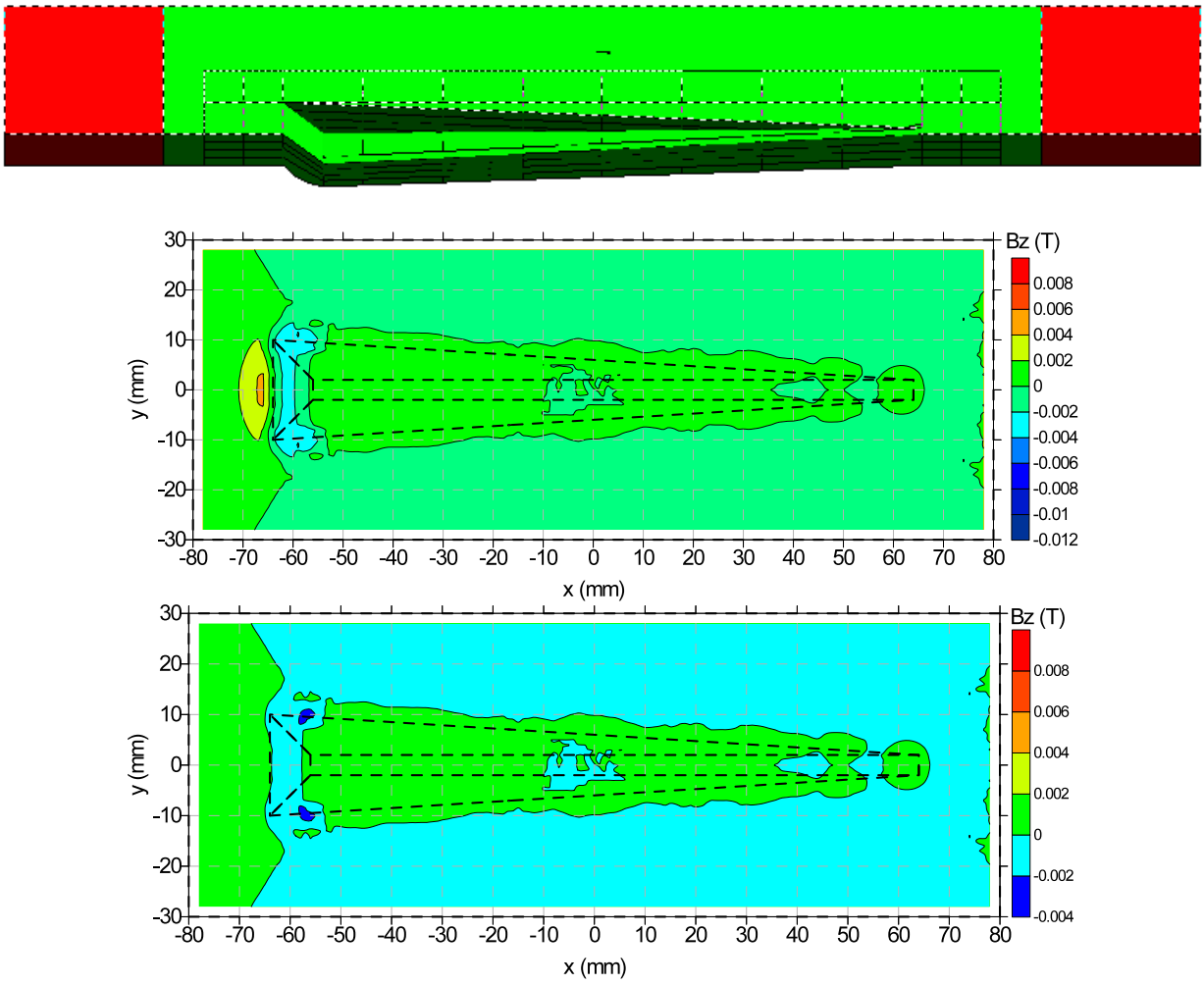

Figure 18. Inner wall radial MFL signal from 'Gouge 2' – 'No sensor liftoff' (top), and 'Sensor liftoff' (bottom). Sensor travels from right to left.

3.2 Experimental Sensor Liftoff Signals

For experimental verification of the modeled liftoff results, measurements were performed on a few representative samples from previous and concurrent projects. The description of the experimental set-up and the samples used is given in Section 2.3. Figure 19 below shows typical axial and radial MFL signal from a circular dent in the presence of sensor liftoff when the detector moves from left to right. The MFL signal at the trailing end is weaker than that on the leading end, and the radial signal is severely affected by the sensor liftoff. These observations agree well with the model predictions. The liftoff signals for axially elongated dent shown in Figure 20 and for circumferentially elongated dent shown in Figure 21 reveal the same information. The central peak in the axial signal in Figure 20 does not split as in the model due to relatively short length of the experimental dent.

The MFL signals for the backhoe dent+gouge used in the present work are shown in Figure 22. Unlike the circular and elongated dents, the signals from this dent+gouge defect do not resemble much with the corresponding modeled signal (Figures 15 and 16). This should not be surprising because an experimental gouge has complex geometry as well as strain pattern, whereas the modeled gouge consists of a smooth geometry and has isotropic material properties. Nevertheless, the effect of signal loss due to liftoff is apparently observable from the axial MFL signal that becomes very weak near the trailing end (right side) of the gouge.

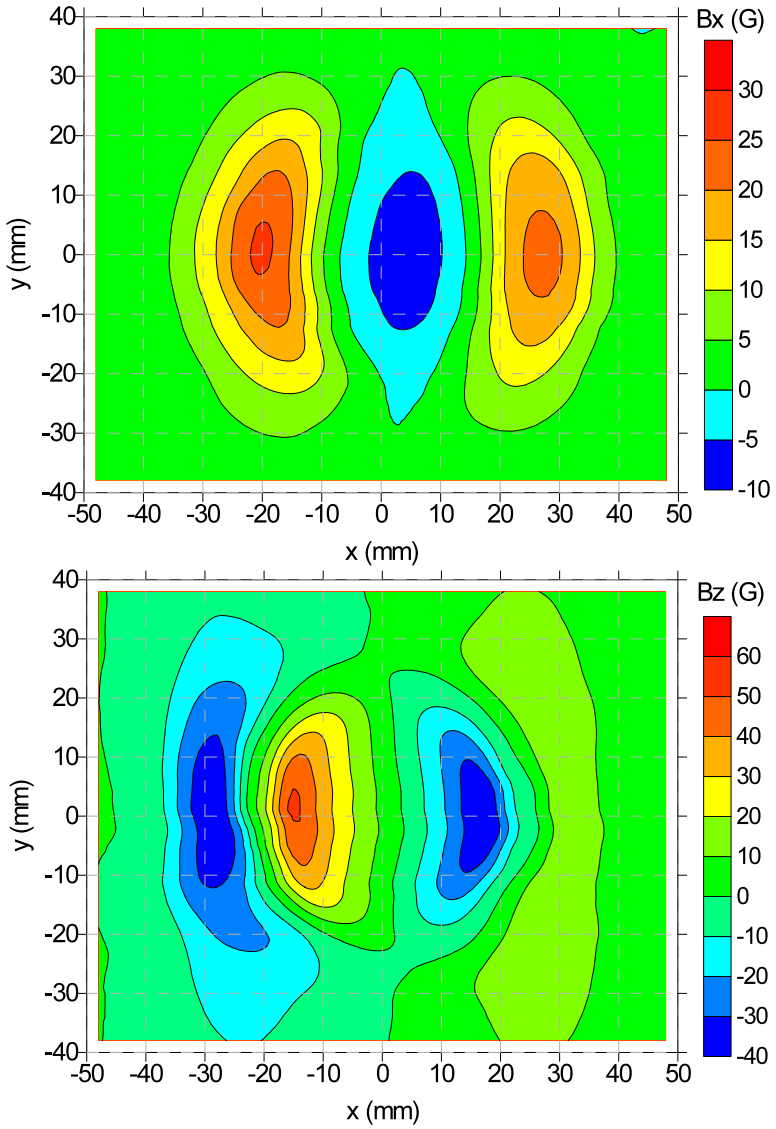

Figure 19. Experimental MFL axial (top) and radial (bottom) signals from a circular dent shown in Figures 3 and 9 in the presence of sensor liftoff. The sensor motion is from left to right.

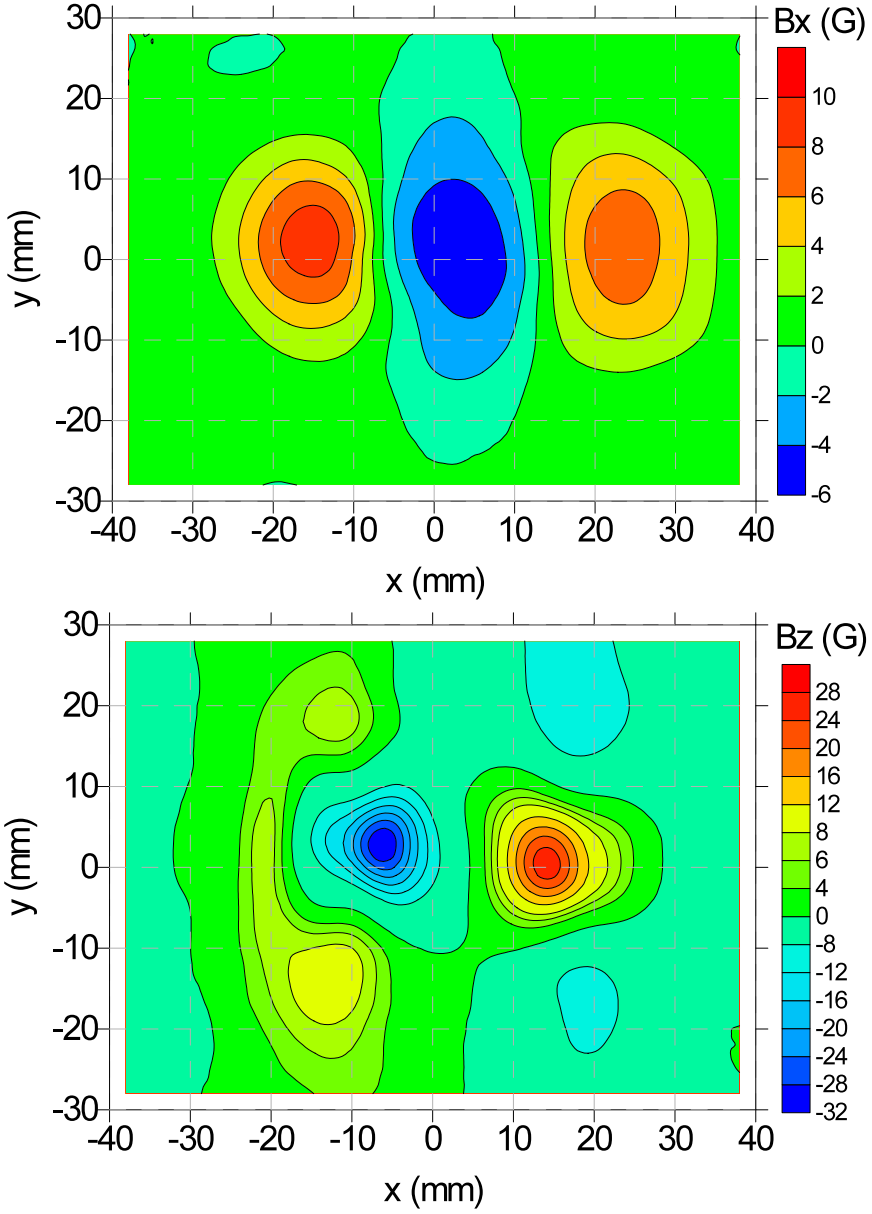

Figure 20. Experimental MFL axial (top) and radial (bottom) signals from an axially elongated dent shown in Figure 5 in the presence of sensor liftoff. The sensor motion is from left to right.

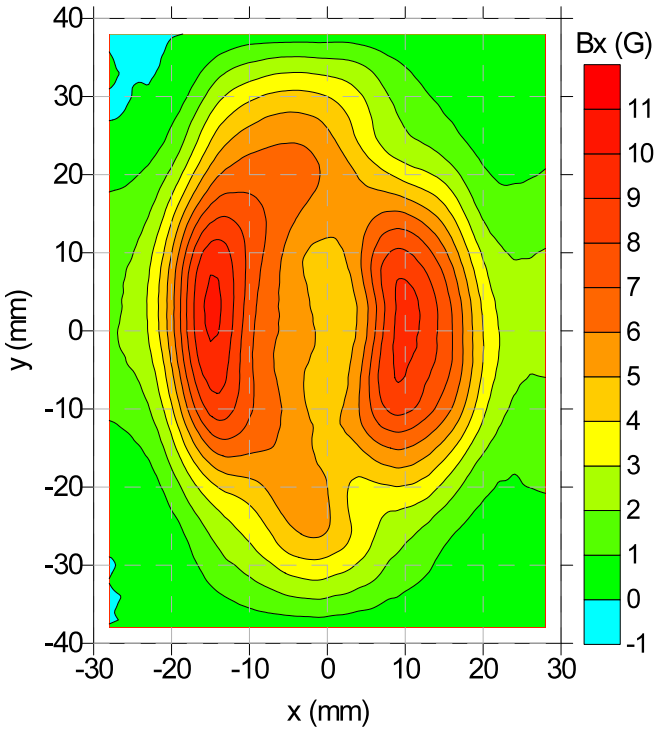
Bx (G)
11
10
9
8
7
6
5
4
3
2
1
0
-1
40
30
20
10
0
-10
-20
-30
-40
y (mm)
-30
-20
-10
0
10
20
30
x (mm)

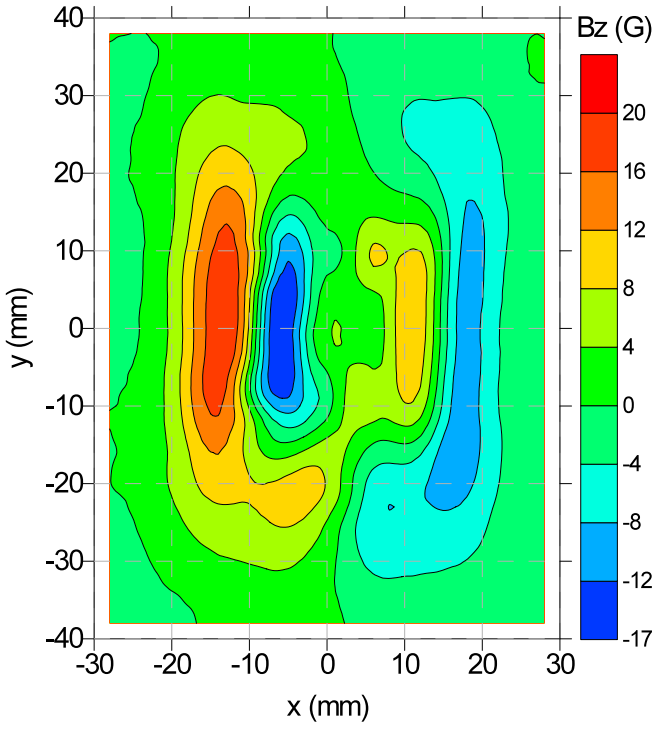
Bz (G)
20
16
12
8
4
0
-4
-8
-12
-17
40
30
20
10
0
-10
-20
-30
-40
y (mm)
-30
-20
-10
0
10
20
30
x (mm)

Figure 21. Experimental MFL axial (top) and radial (bottom) signals from a circumferentially elongated dent shown in Figure 6 in the presence of sensor liftoff. The sensor motion is from left to right.

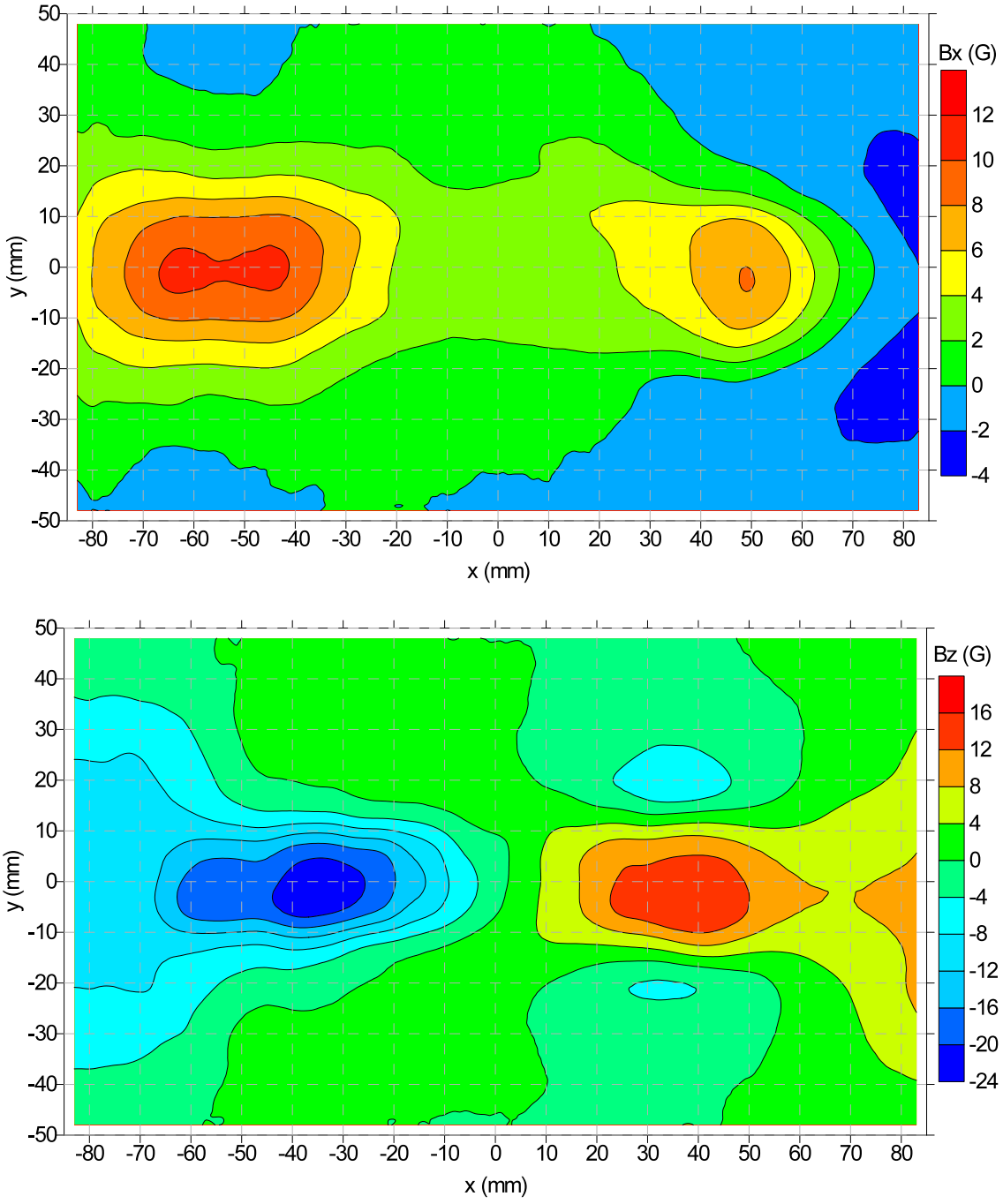

Figure 22. Experimental MFL axial (top) and radial (bottom) signals from the backhoe dent+gouge shown in Figure 7 in the presence of sensor liftoff. The sensor motion is from left to right.